



**HAL**  
open science

# Deep learning-driven palmprint and finger knuckle pattern-based multimodal Person recognition system

Abdelouahab Attia, Sofiane Mazaa, Zahid Akhtar, Youssef Chahir

## ► To cite this version:

Abdelouahab Attia, Sofiane Mazaa, Zahid Akhtar, Youssef Chahir. Deep learning-driven palmprint and finger knuckle pattern-based multimodal Person recognition system. *Multimedia Tools and Applications*, 2022, 81 (8), pp.10961 - 10980. 10.1007/s11042-022-12384-3 . hal-03655718

**HAL Id: hal-03655718**

**<https://hal.science/hal-03655718>**

Submitted on 29 Apr 2022

**HAL** is a multi-disciplinary open access archive for the deposit and dissemination of scientific research documents, whether they are published or not. The documents may come from teaching and research institutions in France or abroad, or from public or private research centers.

L'archive ouverte pluridisciplinaire **HAL**, est destinée au dépôt et à la diffusion de documents scientifiques de niveau recherche, publiés ou non, émanant des établissements d'enseignement et de recherche français ou étrangers, des laboratoires publics ou privés.

# Deep learning-driven palmprint and finger knuckle pattern-based multimodal Person recognition system

Abdelouahab Attia<sup>1,2</sup>  · Sofiane Mazaa<sup>1,2</sup> · Zahid Akhtar<sup>3</sup> · Youssef Chahir<sup>4</sup>

Received: 25 February 2021 / Revised: 19 January 2022 / Accepted: 21 January 2022

Published online: 17 February 2022

© The Author(s), under exclusive licence to Springer Science+Business Media, LLC, part of Springer Nature 2022

## Abstract

Biometric recognition systems are widely being used in several applications due to its distinctiveness and reliability. In recent years, hand-based person recognition has received much momentum due to its stability, feature richness, reliability and higher user acceptability. In this paper, we propose a multimodal hand biometric system based on Finger Knuckle Print (FKP) and Palmprint. In particular, the PCANet deep learning method is employed to extract distinctive features from each modality. Then, multiclass SVM is utilized to compute a matching score for each individual modality. Finally, score level fusion is performed to combine the matching scores via different rules such as, min, sum, max and multiplication. The performance of the proposed system is evaluated on the publicly available database known as PolyU. First, we conducted several experiments on single FKP and Palmprint traits. Next, score level fusion based multimodal experiments were performed. The proposed framework was able to achieve 0.00% of EER (equal error rates) and 100% of rank-1 performance. In addition, the proposed system based on PCANet with score level fusion of FKP and Palmprint outperformed existing multimodal methods.

**Keywords** Finger knuckle print · Palmprint · Score level fusion · PCANet deep learning · SVM multiclass

---

✉ Abdelouahab Attia  
attia.abdelouahab@gmail.com

<sup>1</sup> MSE Laboratory, Mohamed El Bachir El Ibrahimi University, Bordj Bou Arreridj, Algeria

<sup>2</sup> Computer Science Department, Mohamed El Bachir El Ibrahimi University, Bordj Bou Arreridj, Algeria

<sup>3</sup> State University of New York Polytechnic Institute, Utica, NY, USA

<sup>4</sup> Image Team GREYC-CNRS UMR, University of Caen, Caen, France

# 1 Introduction

Biometrics is widely being deployed as a person identification system in several real-world applications [10, 11, 21]. At the same time, biometrics is a rapidly expanding field of research. However, the hand biometric system plays an important role in the security systems. It is being used to identify individuals such as clients and employees in many access control applications [26]. Hand-based biometric system, including Finger Knuckle Print (FKP) and Palmprint, provides reliable, low-cost system, especially because of using small size imaging device requiring extra hardware [7, 9, 25]. The main advantage of palmprint modality is its stability and distinctive characteristics from person to person. Also, palmprint contains huge texture information, which provides a meaningful data for person recognition [14]. While, FKP also has distinctive anatomical structures. FKP has been recently studied to ameliorate biometric authentication system with higher accuracy [12, 29]. It is well-known fact that any unimodal hand biometric systems are not totally ideal to be used in absolute security applications. Unimodal systems are vulnerable to varying environmental situations, sensors' noises, poor quality samples, and spoofing or presentation attacks. Despite remarkable progress, their performance remains insufficient for security applications. To overcome some limitations of unimodal, multi-biometric systems have been devised, i.e., biometric fusion by combining different traits' information provided by individuals that enhances the quality and effectiveness of authentication in biometric systems.

Recently, deep learning methods have been taken substantial consideration in different fields [5, 13, 22, 37] in biometric systems [8, 15, 17]. The basic idea of deep learning used in biometrics is to discover multiple levels of representation, which is based on the discriminant characteristics of biometric modality effectively and efficiently. Deep learning can be used in a biometric system at different steps, i.e., preprocessing of interest region extraction, feature extraction, matching score, matching, and decision. All in all, deep learning in biometrics has been mainly applied for feature extraction. Very limited works have been focused on FKP and palmprint based multimodal systems. Despite current advances, research works on multimodal biometrics system using FKP and palmprint still have some limitations such as they face difficulty and complexity of recognition and lose their simplicity and robustness, and higher FAR and EER rate metrics. It's still a big challenge to avoid all these problems and enhance the recognition performances. However, score level fusion of several modalities such as palmprint and FKP can accurately achieve higher performance than unimodal recognition systems. Moreover, a multimodal biometric system is capable to process a huge number of enrolled templates of an individual in the database. Despite remarkable progress in the multimodal system, hand-based multimodal systems have received less attention. Thus, new hand-based biometrics recognition system using palmprint and FKP needs to be developed to overcome the limitations and decrease the false acceptance rate and EER.

Thus, in this paper, a simple and fast hand-based recognition multimodal biometrics system is proposed using palmprint and FKP modalities at matching score-level fusion. The proposed system uses PCANet deep learning technique and several matching score fusion rules, i.e., multiplication, sum, max, and min rules. Specifically, the Deep Learning Feature Extraction PCANet is used for extract feature from each of the Region of Interest (ROI) of FKP and palmprint images. This process is composed of two stages, i.e., PCA filter bank and binary hashing, in addition to their simplicity, PCANet technique provides a reasonable feature vector size at low processing time, which makes it efficient and attractive choice in several applications such as remote authenticate via internet and real-time applications. Then, the SVM multi-

class classification scheme is employed in matching stage that is followed by scores level fusion of FKP and palmprint. Next, some of the technical rules for fusion score are utilized to obtain the unified score for a final decision. A final decision is made via an evaluation of performance. We use FAR (False Acceptance Rate) and EER (Equal Error Rate) as well as Rank-one metrics to evaluate the accuracy of the proposed system.

The remainder of the article is organized as follows. Section 2 provides the related work on FKP and palmprint biometric system. Section 3 describes the proposed multimodal biometric system. This section presents an overview of the architecture of multimodal biometric system, process of ROI extraction, feature extraction using PCANet, matching based on multi-class SVM to identify person, score level fusion rules, and evaluation criteria of multimodal biometric system. Section 4 presents the different datasets, parameters setting, and experimental results. The conclusion and future work are given in the Section 5.

## 2 Related work

The motivation of this work is to provide biometric system-based FKP and palmprint modalities for more accurately identify a person. In order to develop better systems, we need deeper insights about existing works on FKP and palmprint information fusion. Studies have been conducted to develop different multimodal biometrics, e.g., information fusion of FKP with palmprint traits was explored by Jaswal et al. [27] and Oveisi and Modarresi [32]. Authors in [27] and [32] took the advantages of both modalities to ameliorate the performance compared to system using a single hand biometric modality. Also, other works exist in the literatures that are based on FKP and palmprint. Though most of existing works used different techniques for feature extraction level and variation of fusion schemes, they still suffer in term of false acceptance rate. For example, Zhu et al. [42] have designed a FKP and palmprint information based system with decision level fusion. However, the 'AND' rule has been employed, which is known for generated higher error rates. This method can be used for the supplementary development of an automated security system based on hand modality with large population/database with high performance in terms of, accuracy, robustness, and efficiency.

Jaswal et al. [27] have presented a novel multimodal biometric authentication system using multiple templates (features) of both FKP and palmprint. Their system is based on Random Forest via Kernel-2DPCA. First, fixed size ROIs of traits (palm and FKP) were extracted, then poor contrast ROI images were improved via a modified CLAHE algorithm. Next, the authors use Line Ordinal Pattern (LOP) based transformation in order to minimize the pose and illumination effects. Later, the original feature space is mapped into a high dimensional sub-feature set. In this step, the authors employed K2DPCA method that performed on each subset to extract higher-order statistics. In the matching step Random Forest method has been used. It can be concluded that longitudinal features of the palmprint and FKP modalities are useful and robust than transverse features.

Oveisi and Modarresi [32] combined palmprint and knuckle print images at feature level. The authors intended to propose an effective feature representation based on Dual Tree-Complex Wavelet Transform (DTCWT) that offers both approximate shift invariance and good directional selectivity. However, the goal of this representation is also to better maintain the discriminable features. Thus, it achieves less redundancy and high computational efficiency. AdaBoost classifier has used to resolve the problem of a limited number of training data in

unimodal systems. However, noisy data may impact the performance of the method. Whereas, Meraoumia et al. [30] represented a multiple trait system for person recognition based on palmprint and FKP modalities. The authors used 1D Log-Gabor response for feature extraction from \*two modalities. Then, each image FKP or palmprint is represented by its real and the imaginary templates. Later, each extracted template is compared with those stored in the database via Hamming distance at matching the score level via min rule. This method's performance suffers under a large size database. Perumal and Lakshmi [33] developed a palmprint and FKP based multimodal biometric system by employing Speeded UpRobust Features (SURF) and Empirical mode decomposition (EMD) to extract features. Score level fusion was utilized to merge the matching scores with sum, min, and max rules. It should be highlighted that EMD have limitations such as the stop criterion and the size of the extracted oscillations intrinsic mode functions (IMFs). While, Jaswal and Poonia [24] proposed a FKP and palmprint biometric system using feature selection and score fusion level. The presented system used LOP for texture enrichment and back tracking search algorithm with 2D2LDA to select the dominant plan and knuckle feature for classification. Unsupervised rank level fusion rule combining two modalities was performed by Borda Count Method with Z-score, min-max, and Tanh rules. The main benefit of this method is extraction of the optimal features of both modalities palmprint and finger knuckle. Nigam and Gupta [31] proposed a multi-biometric FKP and palmprint based method for person recognition, where the sign of local gradient (SLG) and sum rule were used for feature extraction and score level fusion, respectively.

Kant and Chaudhary [28] utilized three modalities (i.e., finger knuckle print, fingerprint, and palmprint) to implement a multimodal biometric system. They extracted the features set of each modality, then a fusion at the match score level was executed to increase the recognition accuracy. However, the achieved performance can be ameliorated. Also, Attallah et al. [6] proposed a biometric recognition system that is based on FKP and palmprint. The system uses LBP and BSIF methods for feature extraction and PCA for reducing the dimensionality of the vector that has been provided by the feature concatenation of FKP and palmprint. In the decision step, they used Extreme learning Machine (ELM).The limitations of this system are the use of BSIF descriptor that need selection of the best filter from 56 BSIF filters and use of PCA method as it is characterized by the loss of information. Veluchamy and Karlmarx [38] have used He-Co-HOG method for feature extraction from FKP and Palmprint with Fractional FireFly (FFF) algorithm. FFF was used to obtain the optimal weight score at the feature fusion level. Finally, layered K-SVM classifier was used in the decision step. Regardless of current progress in multimodal system, there is a huge demand of hand-based multimodal systems with higher accuracy. Thus, there is a need of investigation of new model based on deep learning methods [2–4]. Table 1 summarizes the representative prior works.

### 3 Proposed multimodal biometric system

Figure 1 illustrates schema of the proposed multimodal FKP and palmprint biometric system based on PCANet method with score level fusion. The main system steps include (for both palmprint and FKP modalities):

- (i) Extracting Region Of Interest (ROI).
- (ii) Feature extraction by PCANet.

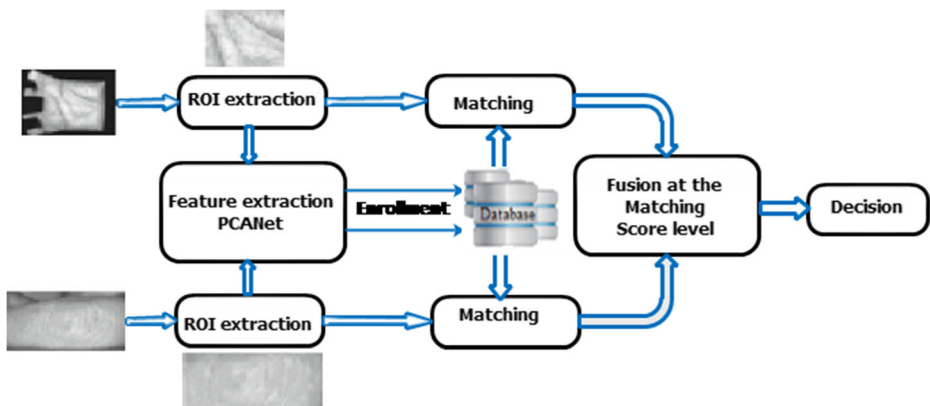
**Table 1** Summary of conventional finger knuckle print and palmprint recognition systems

Authors	Type of fusion	Features extraction	Similarity/Matching
Jaswal et al. [27]	Score level fusion	Kernel-2DPCA	Random Forest
Oveisi and Modarresi [32]	Feature level fusion	DTCWT	AdaBoost classifier
Zhu et al. [42]	Decision level fusion	Sharpe edge features +wavelet	AND rule
Meraoumia et al. [30]	Score level fusion	1D Log-Gabor	Hamming distance/min rule
Perumal and Lakshmi [33]	Score level fusion	SURF + EMD	sum, min, and max rules
Jaswal and Poonia [24]	Feature selection and score fusion level	LOP method for texture enrichment with 2D2LDA	Z-score, min-max, sum-w and Tanh rules
Nigam and Gupta [31]	Score level fusion	Sign of local gradient,	Sum rule
Kant and Chaudhary [28]	Score level fusion	-	Sum rule
Attallah et al. [6]	Feature level fusion	LBP and BSIF PCA for reducing the dimensionality	Extreme learning Machine (ELM)
Veluchamy and Karlmar [38]	Feature level fusion	He-Co-HOG method+ Fractional FireFly (FFF) algorithm	K-SVM classifier

- (iii) Matching process for each single modality(either FKP or palmprint) based multi-class SVM method.
- (iv) Score Fusion of two modalities using different rules such as Multiplication, Min, Sum, and Max). Depending on the individual matching score fusion, the final decision is taken (the individual is accepted as genuine or rejected as impostor).

### 3.1 Region of Interest Extraction (ROI)

The goal of the ROI extraction process is to obtain the only area that contains the useful or discriminative information of input modalities (FKP or palmprint) in order to achieve an

**Fig. 1** Proposed multimodal system

accurate matching. Thus, these subsections describe the ROI extraction process for both biometric modalities FKP and palmprint as follows.

### 3.1.1 Palmprint ROI extraction

The central section of palmprint image is the essential part, which must be extracted [40]. This zone has the boundary of Palmprint that has the global characteristics and allow describing distinctive features. Once the palmprint image is captured, the two holes tangent is poisoned that show the size between four fingers (forefinger, middle finger, ring finger, and the little finger) and used to arrange the palmprint in a line shape. Then, the central area of the palmprint image is cropped for palmprint representation. Therefore, the ROI is defined in a square form and is converted to an image size (128 × 128 pixels). The process of extracting Palmprint ROI is illustrated in Fig. 2.

According to Fig. 2, the process of ROI extraction is performed as in [40] :

- i. Apply a Gaussian smoothing operation to the input image.
- ii. binarize of the smoothed image via a threshold  $h$  (Fig. 2).
- iii. Obtain boundary of the binary image that simply extracted via a boundary-tracking algorithm, as presented in Fig. 2.
- iv. Determine the points lies between fingers for locating the 2D ROI pattern of the boundary image (Fig. 2).
- v. Finally, extract the ROI area.

### 3.1.2 FKP ROI extraction

The main goal of FKP ROI extraction is to determine the rectangle that covers the region of FKP features. This process is considered like a preprocessing step to obtain the useful information of FKP traits. Figure 3 illustrates the process steps to extract the ROI from FKP traits. The procedure as in [41] :

- i. Apply a Gaussian Smoothing operation to the original image (Fig. 3(a)).
- ii. Determine the X-axis of the coordinate system fixed from the bottom boundary of the finger (Fig. 3(b)). So, it extracts the bottom boundary of the finger with the Canny edge detector.
- iii. Determine the Y-axis of the coordinate system that is based on the Canny edge detector on the region (Fig. 3(c)). It has been extracted from the original image on X-axis. This step gives us the location of the convex direction.
- iv. Finally, determine ROI coordinates system, where the rectangle covers the region of information on the ROI.

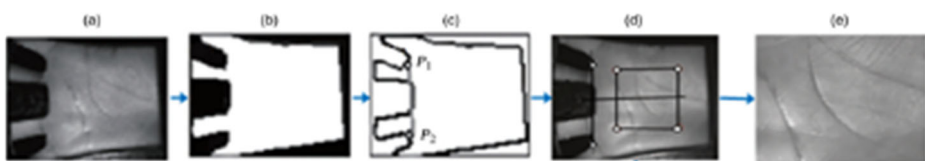


Fig. 2 ROI extraction process of palmprint image

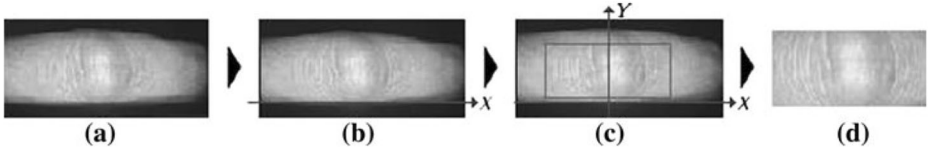


Fig. 3 ROI extraction process of FKP image

### 3.2 Feature extraction

Feature extraction is a significant step in any pattern recognition system because it helps to achieve high performing results. It is important to obtain distinctiveness and unevenness features to differentiate between different patterns [35, 36]. Thus, the PCANet deep learning has been employed, in this study, to extract the feature vector of each FKP and palmprint images.

#### 3.2.1 PCANet deep learning based features

PCANet [16] is a simple deep learning network that it is widely used for feature extraction in image classification. PCANet trains more easily than other deep learning networks, like convolution deep neural network (ConvNet). PCANet is carried out via three basic processing components:

- 1) Cascaded Principal Component Analysis (PCA) to extract high-level features (PCA Filter Bank).
- 2) Binary hashing.
- 3) Histograms.

Feature extraction for both FKP and palmprint modalities using PCANet [16, 39] method is illustrated in Fig. 4. Steps of PCANet are given as follows:

**PCA filter bank** As illustrated in Fig. 4(a and b), the PCA filter bank contains two stages of filter bank convolutions. In the first stage, the filter banks are estimated by running PCA method over filters. The filters consist of a set of vectors, where each vector stands for a small window of the  $k_1 \times k_2$  size around each point (pixel) of each trait FKP or palmprint. Then, the mean of the entries for each vector is taken, and minus the mean of each entry of the vector. Then, PCA is performed on these vectors to retain the principal components ( $W$  of size  $k_1 \times k_2 \times L_{S1}$ ), where  $L_{S1}$  is the primary Eigenvectors. However, each principal component  $W$  is considered as a filter and can be converted to  $k_1 \times k_2$  kernel. This filter has been convolved with the input image as follow:

$$I_1(x, y) = h_1(x, y) * I(x, y), \quad (1)$$

where  $*$  refers to the discrete convolution.  $l \in [1, l_{s1}]$ .  $I$  is the resulting filtered image using the  $h$  filter.

The second stage of PCANet is performed by iterating the algorithm for all output images given from the first stage. The process is, for every output image  $I$ , taking the mean into consideration. Then, removing the mean from each input of the vector computed. Next,



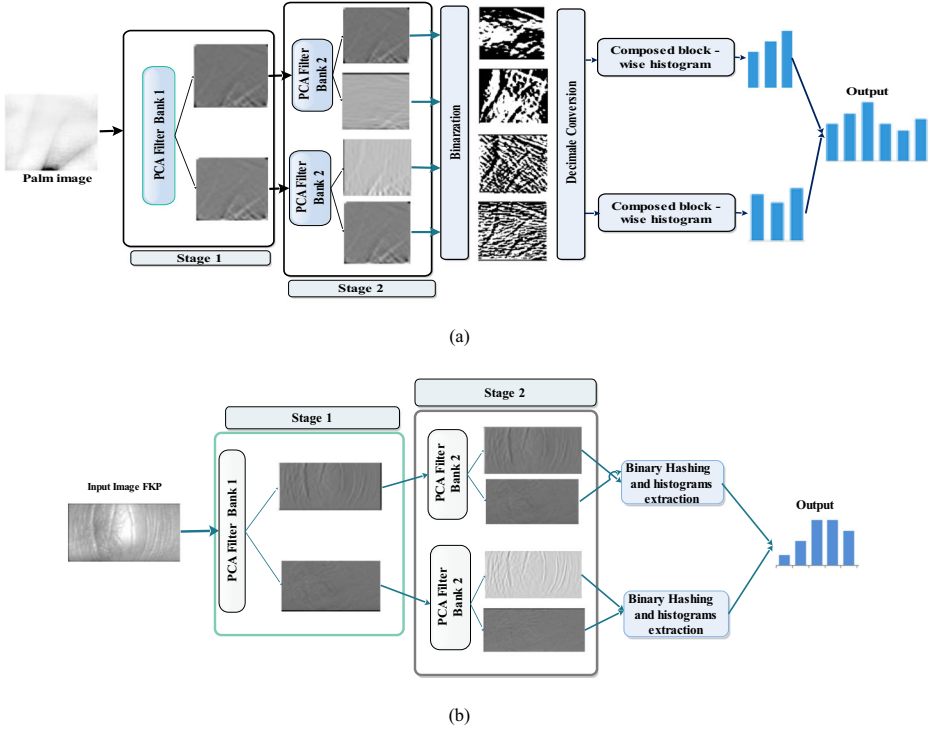


Fig. 4 Scheme of the PCANet deep learning-based feature extraction

concatenating all vectors in one vector and another PCA filter bank (with LS2 filters) is estimated. In the end, every obtained filter is convolved with  $I$  to create a new image.

$$I_{l,m}(x, y) = h_m(x, y) * I_l(x, y),$$

Thus, with repeat convolution step for both filters,  $L_{S1}$  and  $L_{S2}$ , to produce output images by using the output images of the first stage.

**Binary hashing** In this part, the achieved output LS1 and LS2 in the previous step is transformed into binary data by using a Heaviside step function given as:

$$I_{l,m}^B(i, j) = \begin{cases} 1 & \text{if } I_{l,m}(i, j) \geq 0 \\ 0 & \text{otherwise} \end{cases} \quad (2)$$

where  $I_{l,m}^B$  is the binary image. Then, around each pixel, the vector of  $L_{S2}$  binary bits is taken as a decimal number. Thus, we convert the LS2 outputs into a single integer-valued (image).

$$I_l^D(i, j) = \sum_{m=1}^{L_{S2}} 2^{m-1} I_{l,m}^B(i, j) \quad (3)$$

where  $I_l^D$  refer to the hashed image. Each value of pixels is an integer in the range  $[0, 2^{L_{S2}-1}]$ .

**Histogram composition** In this final step, all hashed images  $I_1^D$  are split into NB blocks. Then, the histogram of each block (B) is computed. Note that these blocks can be overlapping or non-overlapping, which depends on the application or disjoint, respectively. As a result, the features extracted from  $I_1^D$  are obtained by associating all blocks histograms B as follows:

$$v_1^{\text{hist}} = [B_1^{\text{hist}}, B_2^{\text{hist}}, \dots, B_{\text{NB}}^{\text{hist}}] \quad (4)$$

After the encoding step, the feature vector of the input image I is then concatenated as follows:

$$v_I^{\text{hist}} = [v_1^{\text{hist}}, v_2^{\text{hist}}, \dots, v_{L_{S1}}^{\text{hist}}] \quad (5)$$

### 3.2.2 Parameters of PCANet

Before, we perform PCANet deep learning to extract the significant features. We must define their parameters. The parameters of the PCANet, including the number of filters in each stage ( $L_{S_i}$ ), the filter size ( $k_1; k_2$ ), the number of stages (Ns), as well as the block size for local histograms in the output layer (B). Evaluation of the performance of the introduced system based on PCANet involves initializing these parameters. These parameters are very important to generate the best features that represent an input FKP or palmprint traits. Also, they are very interesting to improve the performance of the recognition system. These parameters are empirically selected and are depicted in Table 2.

### 3.2.3 Computational complexity of PCANet [16]

The PCANet is efficient both in its performance and computational complexity. The light computational complexity of PCANet method can be seen as the patch-mean-removed matrix X costs  $k_1k_2 + k_1k_2mn$  flops, the Eigen-decomposition step has complexity of  $O((k_1k_2)^3)$ , the complexity of the inner product  $XX^T$  is of  $2(k_1k_2)^2mn$  flops. In each stage, the PCA filter convolution takes  $L_{S_i}k_1k_2mn$  flops. In the output layer, the conversion of binary bits to a decimal number of  $L_{S_2}$  takes  $2L_{S_2}mn$ , and the naive histogram operation has complexity of  $O(mnBL_{S_2} \log 2)$ . Assuming  $mn \gg \max(k_1; k_2; L_1; L_2; B)$ , the overall complexity of PCANet is easy to be verified as  $O(mnk_1k_2(L_{S_1} + L_{S_2}) + mn(k_1k_2)^2)$ . Generally, the training time of CNNs (ConvNet) is longer than PCANet. In fact, the training of PCANet on around 100,000 images of  $80 \times 60$  pixel size just takes 30 minutes, but CNN-2 takes 6 h [16].

**Table 2** PCANet parameters both modalities FKP and palmprint

FKP	Palmprint
The Number of Stages = 2	The Number of Stages = 2
The number of filters = [7 7]	The number of filters = [7 7]
The filter size = [4 4]	The filter size = [4 4]
The block size = [21 21]	The block size = [7 7]
The overlapping = 0.5%	The overlapping = 0.5%

### 3.3 Support vector machines

Vapnik and Cortes introduced Support Vector Machine (SVM) [19] as a supervised learning method that classifies data by drawing a set of support vectors. SVM is a powerful classifier algorithm that has been used in different areas, including biometrics systems. Generally, SVM generates a hyper-plane between two sets of data for classification. The basic idea of SVM algorithm is based on kernel functions via solving a quadratic optimization problem to separate data into different groups. As a result, the SVM method generates the optimal hyperplane with the largest margin. In other words, SVM project data into another higher-dimensional space. Then, SVM traces the optimal hyperplane in the projection space [19]. In this work, multi-class SVM has been applied. Multiclass SVM generated 165 classes (individuals) to authorize individual using modality FKP and palmprint. For all 165 subjects, each one of them has 6 FKP and 6 palmprint feature vectors for classification. In other words, every feature vector consists of a unique image of FKP image type (LIF, LMF, RIF, and RMF) and palmprint image. Then, SVM finds the hyperplane that separates the largest possible between two or more sets of the object (points of the same class on the same side), though maximizing the distance from either class to the hyperplane.

### 3.4 Score level fusions rules

Fusion at the matching score level is a commontechnique that has been widely used because of its simplicity [25]. The outputs of the two matching modules FKP and palmprint are combined using fusion rules. The goal is to merge the outputs scores in order to generate a single score  $S$  that will be used in the process of decision making. Such fusion techniques are expressed by multiplication, min, max and sum rules.

$$\textit{Multiplication} : S = \prod_{i=1}^N S_i \quad (6)$$

$$\textit{Min} : S = \min(S_i) \quad (7)$$

$$\textit{Max} : S = \max(S_i) \quad (8)$$

$$\textit{Sum} : S = \text{sum}(S_i) \quad (9)$$

Where  $S_i$  is the score of modality  $i$ . The results of such rules are used to compute evaluation metrics, described in the next subsection, which used to make the decision of rejecting or accepting the person.

### 3.5 Evaluation criteria

The evaluation of biometric recognition systems can be performed through two measures [18]:

- 1) FAR (False Acceptance Rate): It refers to the ratio of the number of instances of impostors to total number of impostor attempts.

$$FAR(\%) = (Number\ of\ successful\ impostor\ attempts / Total\ Number\ of\ impostor\ attempts) * 100\% \quad (10)$$

- 2) False Reject Rate (FRR): It refers to the ratio genuine attempts rejected to the total number of genuine attempts.

$$FRR(\%) = (Total\ Number\ of\ false\ rejection / Number\ of\ all\ genuine\ attempts) * 100\% \quad (11)$$

It is noticeable that the system can be adjusted by changing the values of these two criteria (FAR and FRR) for a particular application. However, increasing one of them involves decreasing the other and vice versa. In addition, the EER criteria value has been obtained. i.e., when FAR = FRR.

Furthermore, Receiver Operating Characteristics (ROC) and Cumulative Match Curves (CMC) curve are used to illustrate the performance of biometrics systems. A ROC curve explains how the FAR values are changed compared to the values of the Genuine Acceptance Rate (GAR) [23].

$$GAR(\%) = 100 - FRR(\%) \quad (12)$$

A CMC curve is used in closed-set identification task. CMC presents the accuracy performance of a biometric system and it shows how frequently the individuals' template appears in the ranks based on the match rate.

## 4 Experimental results

In this section, we describe the experimental results of the presented multimodal biometric system using FKP and palmprint. Firstly, we explain the datasets and their different parameters used in the experiments. Then, we give the evaluation results of FPK and Palmprint as unimodal model. Next, we present the evaluation results of proposed multimodal FPK-Palmprint system with the interpretations of their fusion at the matching score level. Finally, a comparison of proposed multimodal FPK-Palmprint with existing studies is presented.

### 4.1 Databases and parameters setting

In order to evaluate the performance of the proposed multi-biometric recognition scheme, several experiments have been carried out on the multi-biometric database that are provided by the Hong Kong Polytechnic University (PolyU- palmprint database [20] and the PolyU FKP

database [34]. FKP database consists of 12 images for each finger per subject with a total of 165 subjects. We randomly selected six samples of each FKP to compose the FKP training set. As a result, the rest of the FKP samples are kept for the test stage. The palmprint database consists of 20 palmprint images per subject with a total of 200 subjects. We randomly selected (165 subjects with 12 samples). Then, we chose six samples of each person to build the palm training set. As a result, the rest of the samples are kept for palmprint test step. It is worth noting that the identification happens when the biometric system tries to detect the identity of a person.

## 4.2 FKP results

In the verifying process, the objective is to check the input template (feature vector) is matched up to only with the features stored in the database of the claimed individual. For FKP modality, we use a single FKP images LIF, LMF, RIF, and RMF to accomplish the verification experiments. In this experiment, six images of each FKP modality were randomly elected to construct a training data (enrollment). While, the rest of the images constructed the test data. As a result, there were 990 training images and 990 test images. Thus, a number of comparisons are a 990 of genuine and 162,360 of impostors. The verification performances of the four modalities (LIF, LMF, RIF, and RMF) are presented in Fig. 5; Table 3.

In Fig. 5(a) (EER) and Table 2 (EER, rank-one recognition rate), we can see that LMF finger modality achieves an accuracy of 97.58% compared to the rest of modalities finger RMF, RIF, and LIF that reached 95.45%, 95.25%, and 96.26%, respectively. Furthermore, in term of EER, LIF finger modality obtained an EER (1.50%) than the other modalities RMF, RIF and LMF reaching 2.12%, 2.22%, and 1.62%, respectively. Therefore, we can say LMF and LIF are more effective to attain higher biometric recognition.

Figure 5(b) (ROC plot), Fig. 5(c) (CMC curves) and Table 2 (verification mode) illustrate that for finger uni-modality is better for LMF and LIF. We can see that LMF achieves a best accuracy rank-one recognition rate than LIF, RMF, and RIF. According to CMC curves and ROC plot, it can be stated that LMF achieves a higher performance. In addition, when we compare LMF with LIF, RMF, and RIF on verification at 0.1% and verification rate at 1%, we find LMF attained accuracy(98.28% and 96.77%) better than other modalities RMF, RIF, and LIF with (96.97%, 95.15%), (96.87%, 94.95%), and (98.18%, 95.05%) accuracies, respectively. Thus, we can say LMF outperformed the RMF, RIF, and LIF finger modalities.

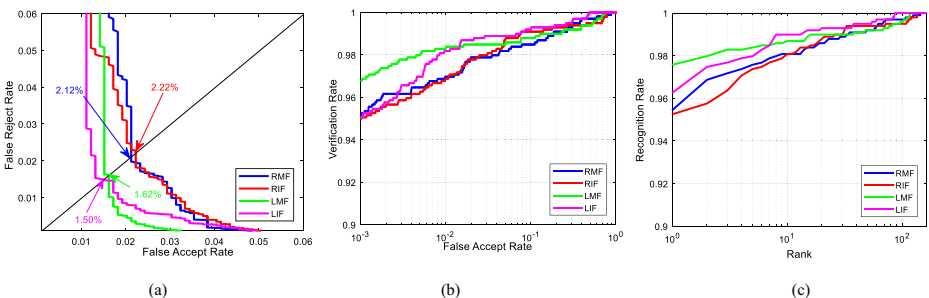


Fig. 5 FKP results a) EER, b) ROC plots, c) CMC curves

**Table 3** Performance for different fingers

modalities	Mode identification	Mode verification		
	Rank-one	EER	VR@1%FAR	VR@0.1% FAR
RMF	95.45%	2.12%	96.97%	95.15%
RIF	95.25%	2.22%	96.87%	94.95%
LMF	97.58%	1.62%	98.28%	96.77%
LIF	96.26%	1.50%	98.18%	95.05%

### 4.3 Palmprint result

According to the Table 4, we can say that the proposed system using a palmprint single modality achieves a high performance reaching to EER = 0.91%. Also, the verification rate at 1% FAR and 0.1% FAR reached 99.09% and 98.09%, respectively. Further, Rank-one accuracy in verification mode achieved 98.38%.

Moreover, Fig. 6 illustrates EER, ROC, and CMC plots that confirm the high-performance results of the proposed system with one single modality (i.e., palmprint). As we see in Fig. 6(a) that EER is 0.91%. Also, the ROC in Fig. 6(b) shows that the palmprint recognition system can quite accurately identify the people, as the GAR = 98.38%. Similarly, CMC plot in Fig. 6(c) confirms the higher capability of the system, namely ranks-one recognition rate achieved 98.38%.

The main reason of obtained high-performance results by the two single modalities of FKP or palmprint is use of PCANet deep learning in the feature extraction step. PCANet deep learning allows extracting the significant features that ensure the best presentation and extraction of data from images.

### 4.4 Multi-biometrics by combining FKP and palmprint

In this section, we present the results of the proposed hand biometrics system combining FKP and palmprint. The respective matching scores of FKP and palmprint obtained by multi-class SVM classifier are fused via four techniques rules (Multiplication, Max, Min, and Sum). To demonstrate the efficiency of the proposed system, we performed all possible combinations of FKP fingers with palmprint modality, i.e., the fusion of each FKP(RIF, RMF, LIF, and LMF) modalities with palmprint modality at the score level. Table 5 illustrates the performance results of proposed hand biometrics system. We can see in Table 4 all possibilities of FKP and palmprint with their fusion rules used. It can be observed in Table 5 all possibilities using FKP and palmprint (i.e., LIF+Palmprint, LMF+Palmprint, RIF+Palmprint, and RMF+Palmprint) to analyze high performance situation.

**Table 4** Performance palmprint

modality	Mode Identification	Mode Verification		
	Rank-one	EER	VR@1%FAR	VR@0.1% FAR
Palmprint	98.38%	0.91%	99.09%	98.79%

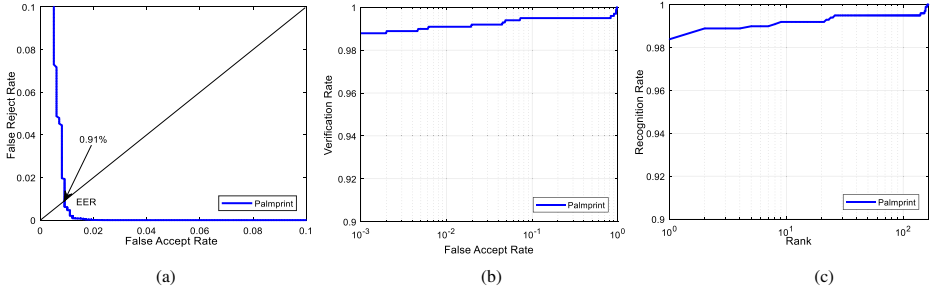


**Fig. 6** Performance palmprint. **a)** EER, **b)** ROC, and **c)** CMC plots

The ROC and CMC plots from all fusion cases (of FKP and palmprint) with all rules are illustrated in Figs. 7, 8, 9, and 10. In these plots, we can observe that the performance of the fusion yielded better performance than the single modalities either FKP or palmprint.

In Table 4, it can be seen that LIF+Palmprint with Mul and Sum fusion rules achieved 100% accuracy in Rank-1 and 0.10% EER. For Min and Max rules, LIF+Palmprint obtained decreased performance, i.e., Rank-1 with 99.80% (0.1%EER) and 98.08% (1.41%EER). Moreover, we can notice that LIF+Palmprint modalities got 100% on VR@1%FAR measure with all fusion rules (Mul, Min, and Sum), except with Max rule that attained 98.48%. Figure 7 show the ROC and CMC of LIF+Palmprint modalities confirming the same. For LMF+Palmprint (in Table 4), it achieved 100% accuracy in Rank-1 and 0.00% EER, 100% VR@1%FAR, and 100% VR@0.1%FAR measures in all fusion rules (i.e., Mul, Min, Sum), except Max rule that achieved 97.98%, 1.71%, 98.08%, and 97.68%, respectively. In addition, Fig. 8 ROC and Fig. 8 CMC plots illustrate high performance of LMF+Palmprint with three fusion rules and little degradation using Max rule.

Further, in Table 5, RIF+Palmprint attained 100% rank-1 accuracy, 0.00% EER, 100% VR@1%FAR, and 100% VR@0.1%FAR for Mul, Min, Sum fusion rules, while Max rule achieved 97.88%, 1.42%, 98.38%, and 97.47%, respectively. In addition, Fig. 9's ROC and Fig. 9's CMC plots show the high performance of LMF+Palmprint with three fusions rules, and not match degradation with Max rule. Whereas, RMF+Palmprint has similar results like LMF+Palmprint and RIF+Palmprint with three fusion rules (Mul, Min, Sum) with 100% rank-

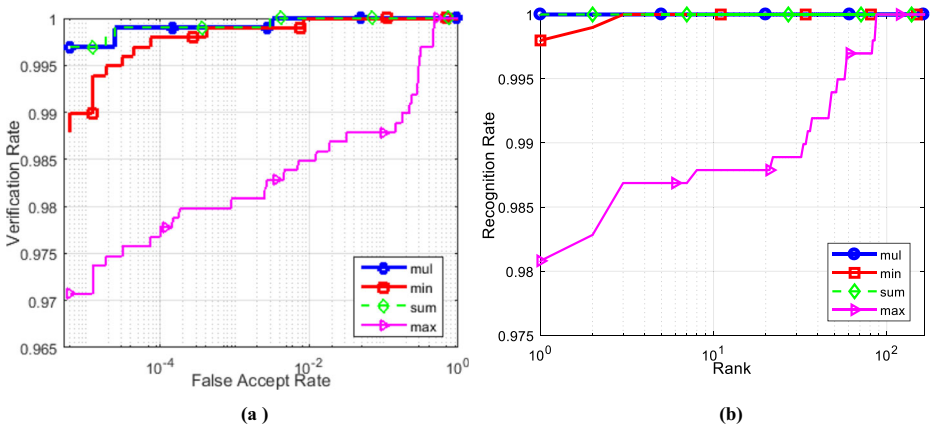


**Fig. 7** LIF-palmprint results of different fusion rules **(a)** ROC curves **(b)** CMC curves

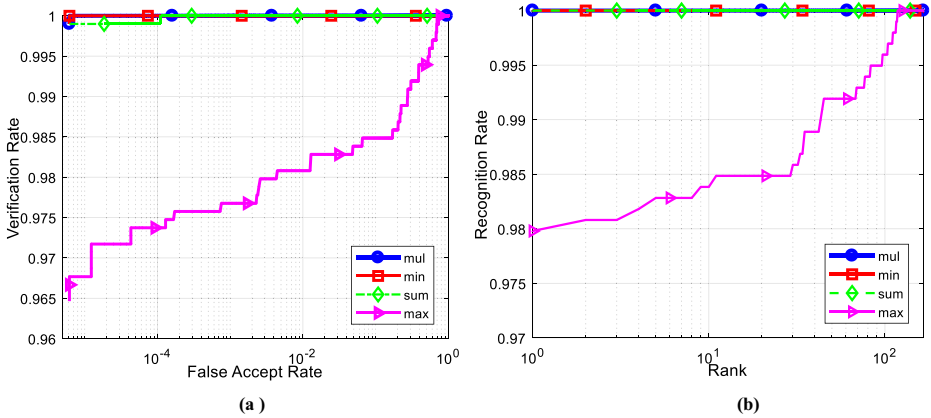


**Fig. 8** LMF-palmprint results of different fusion rules (a) ROC curves (b) CMC curves

1 accuracy, 0.00% EER, 100% VR@1%FAR, and 100%VR@0.1%FAR. For Max rule fusion, there is a very slight drop in accuracy, i.e., 97.78%, 2.02%, 97.88%, and 97.17%, respectively. Figure 10(a) ROC and Fig. 10(b) CMC plots show illustrate the high performance of LMF+ Palmprint with three fusion rules and very small decrease for Max rule. The ROC and CMC graphs for FKP+Palmprint, LMF+Palmprint, RIF+Palmprint, and RMF+Palmprint are illustrated in Figs. 8, 9, and 10(a),(b) using Mul, Sum, and Min, which demonstrate better performance than Max fusion rule. Also, LIF+Palmprint with two fusion rules (i.e., Mul and Sum) that achieved a higher performance, as shown in Fig. 7, compared to Min and Max fusion rules. According to the Table 5, ROC plots, and CMC curves in Fig. 10, the proposed hand-based multimodal biometric system using FKP and Palmprint extensively enhanced accuracy by fusion at the match score level with Mul, Sum, Min, and Max rules, compared to respective individual FKP or palmprint modality. The proposed hand recognition multimodal biometrics system achieved 100% rank-1 accuracy, 0.00% EER, 100% VR@1%FAR, and 100%VR@0.1%FAR in all fusion rules. One of the main reasons for higher accuracies is the PCANet Deep Learning that allows getting significant features.

While our proposed method based on PCANet feature extraction method for both FKP and palmprint modalities, and score level fusion by min, sum, max and multiply rules produces

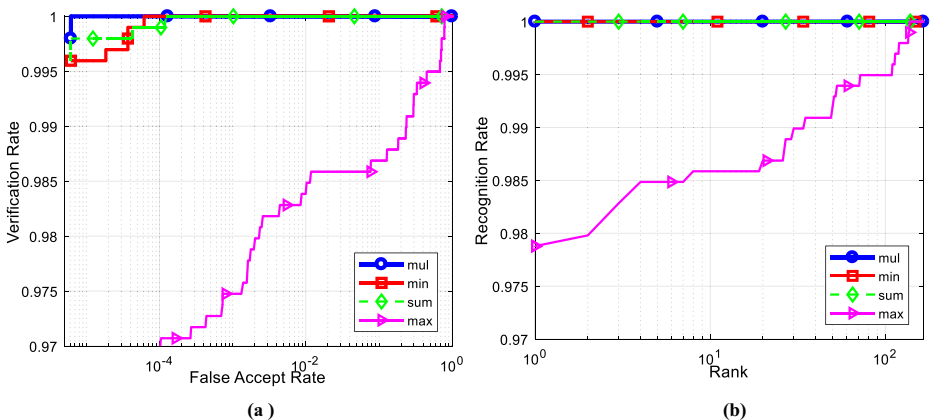


**Fig. 9** RIF-palmprint results of different fusion rules (a) ROC curves (b) CMC curves



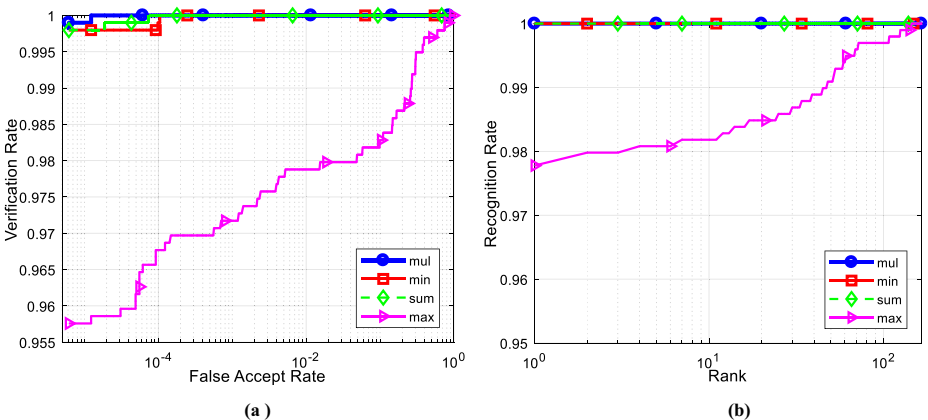
**Table 5** Performance palmprint FKP fusion

modality	Fusion rule	Mode Identification	Mode Verification		
		Rank-1	EER	VR@1%FAR	VR@0.1% FAR
LIF +palmprint	mul	100.00%	0.10%	100.00%	99.90%
	min	99.80%	0.10%	100.00%	99.90%
	sum	100.00%	0.10%	100.00%	99.90%
	max	98.08%	1.41%	98.48%	98.08%
LMF +palmprint	mul	100.00%	0.00%	100.00%	100.00%
	min	100.00%	0.00%	100.00%	100.00%
	sum	100.00%	0.01%	100.00%	100.00%
	max	97.98%	1.71%	98.08%	97.68%
RIF +palmprint	mul	100.00%	0.00%	100.00%	100.00%
	min	100.00%	0.00%	100.00%	100.00%
	sum	100.00%	0.00%	100.00%	100.00%
	max	97.88%	1.42%	98.38%	97.47%
RMF +palmprint	mul	100.00%	0.00%	100.00%	100.00%
	min	100.00%	0.01%	100.00%	100.00%
	sum	100.00%	0.00%	100.00%	100.00%
	max	97.78%	2.02%	97.88%	97.17%

excellent results. However, the proposed method shows some performance limitations in identification mode. It is also notable that accuracy of the system depends on the number of filters, which hugely affects/limits the construction of the final features vectors of FKP or palmprint images. Moreover, the size of the filters manages the mixture of low and high frequency components in the filter bank.

#### 4.5 Comparison with existing FKP palmprint recognition system

In this section, we present the performance comparison of the proposed hand-based multi-modal biometrics system with some well-known prior works to illustrate the effectiveness. These comparisons are made in both modes, i.e., under verification mode with the EER and under identification mode with the rank-1 performances. Table 6 illustrates the effectiveness of proposed system based on FKP and Palmprint score level fusion based PCANet. In Table 6,

**Fig. 10** RMF-palmprint results of different fusion rules (a) ROC curves (b) CMC curves

**Table 6** Comparison of our system multimodal with other existing systems

Ref.	Modality	Feature Extraction/ Fusion Level	Scores Level Fusion rule	Identification Mode	Verification Mode		
					Rank-one	EER	VR@1%FAR VR@0.1% FAR
[30]	RIF +palmprint	Log Gabor	Min	99.85%	0.222%	-	-
[33]	FKP + palmprint	SURF+EMD	Sum	99.68%	0.0744%	-	-
[32]	FKP +palmprint	(DT-CWT)	Min	99.42%	0.035%	100.00%	100.00%
			Max	99.56%	0.39%	98.10%	99.56%
			Min	99.56%	0.39%	98.10%	99.56%
[27]	FKP + palmprint	K2DPCA	sum	99.56%	0.39%	98.10%	99.56%
[38]	FKP + palmprint	Feature level fusion (He-Co-HOG)	Sum-w K-SVM	100.00%	0.68%	-	-
[42]	FKP + palmprint	Local descriptors	-	GAR=99.43%	FAR=0.17%	-	-
[6]	FKP + palmprint	Feature level fusion (BSIF + LBP) with PCA	-	-	0.49%	-	-
[24]	FKP + palmprint	LOP method for texture enrichment with 2D2LDA	Sum-w	100.00%	0.262%	-	-
Proposed Multi-modal System	RIF +palmprint	PCANet	Mul	100.00%	0.00%	100.00%	100.00%
			Min	100.00%	0.00%	100.00%	100.00%
			Sum	100.00%	0.00%	100.00%	100.00%

we can observe that the proposed system obtained a higher accuracy of rank-one equal to 100% and 0.00% EER, which is better than results achieved by well-known recent works. For example, the methods in [27] and [24] achieved 0.68% ,0.262 of EER. Work in [30] and [38] attained lower accuracy rates and EER, i.e., (99.85% and 0.222%), (95.00% and 0.1%), respectively. Whereas, the framework in [6] reached just 0.49% EER. Furthermore, it can be noticed that the works in [32] and [33] achieved accuracy 99.68%, 99.42%,99.56% respectively. Further, the proposed hand recognition multimodal biometrics system achieved 100% VR@1%FAR, and 100%VR@0.1%FAR in all fusion rules. All in all, the proposed system outperformed the existing methods. All in all, one of the main reasons for the proposed method performing well is that it is inspired and based on deep learning techniques, thereby capable of obtaining quite distinctive feature representations.

## 5 Conclusions

In this paper, a multimodal hand biometric system has been proposed, which is based on score level fusion of FKP and Palmprint. The proposed system uses PCANet for feature extraction, SVM multiclass classification scheme for the matching process and four score fusion rules (i.e., multiplication, sum, max, and min) for final decision whether the user is genuine or impostor. The study shows the PCANet can generate highly robust that efficient features from FKP or palmprint images. The proposed system was tested on a public PolyU database that is provided by the Hong Kong Polytechnic University for both traits FKP and palmprint. Two kinds of experiment were presented (i) single modality and (ii) multimodal system with all combinations of FKP and palmprint. In multimodal scenarios, several rules (multiplication, min, sum, max) were analyzed at the matching score level. The experimental results demonstrated that fusion at the matching score level enhances the performance unimodal systems. Also, in comparison with prior existing methods, proposed system achieved the best results. In future work, we will investigate other biometric modalities with similar feature extraction techniques, including methods such as Convolutional Neural Networks (CNNs) and encoder-decoder models. Also, we will revisit multimodal biometric systems to improve their robustness against spoofing attacks, as they have shown to be vulnerable [1] .

## Declarations

**Conflict of interest** The authors declare that they have no conflict of interest.

## References

1. Akhtar Z, Fumera G, Marcialis GL, Roli F (2011) Robustness analysis of likelihood ratio score fusion rule for multimodal biometric systems under spoof attacks. In: Carnahan Conference on Security Technology, pp 1–8
2. Ali A, Zhu Y, Chen Q, Yu J, Cai H (2019) Leveraging spatio-temporal patterns for predicting citywide traffic crowd flows using deep hybrid neural networks. In: IEEE 25th International Conference on Parallel and Distributed Systems (ICPADS), pp 125–132
3. Ali A, Zhu Y, Zakarya M (2021) A data aggregation based approach to exploit dynamic spatio-temporal correlations for citywide crowd flows prediction in fog computing. *Multimed Tools Appl* 80(20):31401–31433

4. Ali A, Zhu Y, Zakarya M (2021) Exploiting dynamic spatio-temporal correlations for citywide traffic flow prediction using attention based neural networks. *Inf Sci (Ny)* 577:852–870
5. Ali A, Zhu Y, Zakarya M (2022) Exploiting dynamic spatio-temporal graph convolutional neural networks for citywide traffic flows prediction. *Neural Netw* 145:233–247
6. Attallah B, Brik Y, Chahir Y, Djerioui M, Boudjelal A (2019) Fusing Palmprint, Finger-knuckle-print for Bi-modal Recognition System Based on LBP and BSIF. In: 6th International Conference on Image and Signal Processing and their Applications (ISPA), pp 1–5
7. Attia A, Chaa M, Akhtar Z, Chahir Y (2020) Finger knuckle patterns based person recognition via bank of multi-scale binarized statistical texture features. *Evol Syst* 11(4):625–635
8. Attia A, Akhtar Z, Chalabi NE, Maza S, Chahir Y (2021) Deep rule-based classifier for finger knuckle pattern recognition system. *Evol Syst* 12(4):1015–1029
9. Attia A, Akhtar Z, Chahir Y (2021) Feature-level fusion of major and minor dorsal finger knuckle patterns for person authentication. *Signal Image Video Process* 15(4):851–859
10. Bastanfard A, Karam H, Takahashi H, Nakajima M (2002) Simulation of human facial aging and skin senility (Session1 Computer Graphics)(IWAIT2002). In: ITE Technical Report 26.3, pp 1–7
11. Bastanfard A, Bastanfard O, Takahashi H, Nakajima M (2004) Toward anthropometrics simulation of face rejuvenation and skin cosmetic. *Comput Animat Virtual Worlds* 15:3–4
12. Benmalek M, Attia A, Bouziane A, Hassaballah M (2022) A semi-supervised deep rule-based classifier for robust finger knuckle-print verification. *Evol Syst* :1–12
13. Bhattacharya S et al (2021) Deep learning and medical image processing for coronavirus (COVID-19) pandemic: A survey. *Sustain Cities Soc* 65:102589
14. Chaa M, Boukezzoula N-E, Attia A (2017) Score-level fusion of two-dimensional and three-dimensional palmprint for personal recognition systems. *J Electron Imaging* 26(1):13018
15. Chaa M, Akhtar Z, Attia A (2019) 3D palmprint recognition using unsupervised convolutional deep learning network and SVM classifier. *IET Image Process* 13(5):736–745
16. Chan T-H, Jia K, Gao S, Lu J, Zeng Z, Ma Y (2015) PCANet: A simple deep learning baseline for image classification? *IEEE Trans image Process* 24(12):5017–5032
17. Chlaoua R, Meraoumia A, Aiadi KE, Korichi M (2019) Deep learning for finger-knuckle-print identification system based on PCANet and SVM classifier. *Evolving Systems* 10(2):261–272
18. Connie T, Teoh A, Goh M, Ngo D (2003) Palmprint recognition with PCA and ICA. In: *Proc Image and Vision Computing, New Zealand*
19. Cortes C, Vapnik V (1995) Support-vector networks. *Mach Learn* 20(3):273–297
20. Database PolyUP, Database “PolyUP (2011) ” [Online]. Available: <http://www.comp.polyu.edu.hk/biometrics/palmprint.htm>
21. Dehshibi MM, Bastanfard A (2010) A new algorithm for age recognition from facial images. *Sig Process* 90(8):2431–2444
22. Gadekallu TR, Rajput DS, Reddy M, Lakshmana K, Bhattacharya S, Singh S ... Alazab M (2021) A novel PCA-whaleoptimization-based deep neural network model for classification of tomato plant diseases using GPU. *J Real-Time Image Process* 18(4):1383–1396
23. Jain AK, Ross A, Prabhakar S (2004) An introduction to biometric recognition. *IEEE Transactions on circuits and systems for video technology*, 14(1):4–20
24. Jaswal G, Poonia RC (2021) Selection of optimized features for fusion of palm print and finger knuckle-based person authentication. *Expert Syst* 38(1):e12523
25. Jaswal G, Kaul A, Nath R (2016) Knuckle print biometrics and fusion schemes—overview, challenges, and solutions. *ACM Comput Surv* 49(2):34
26. Jaswal G, Nigam A, Nath R (2017) DeepKnuckle: revealing the human identity. *Multimed Tools Appl* 76(18):18955–18984
27. Jaswal G, Kaul A, Nath R (2017) Palmprint and finger knuckle based person authentication with random forest via kernel-2DPCA. In: *International Conference on Pattern Recognition and Machine Intelligence*, pp 233–240
28. Kant C, Chaudhary S (2021) A multimodal biometric system based on finger knuckle print, fingerprint, and palmprint traits. In: *Innovations in Computational Intelligence and Computer Vision*. Springer, Berlin, pp 182–192
29. Lakshmanan S, Vellian P, Attia A, Chalabi NE (2022) Finger knuckle pattern person authentication system based on monogenic and LPQ features. *Pattern Anal Appl*: 1–13
30. Meraoumia A, Chitroub S, Bouridane A (2011) Palmprint and Finger-Knuckle-Print for efficient person recognition based on Log-Gabor filter response. *Analog Integr Circuits Signal Process* 69(1):17–27
31. Nigam A, Gupta P (2015) Designing an accurate hand biometric based authentication system fusing finger knuckleprint and palmprint. *Neurocomputing* 151:1120–1132

32. Oveysi IS, Modarresi M (2015) A feature level multimodal approach for palmprint and knuckleprint recognition using AdaBoost classifier. In: International Conference and Workshop on Computing and Communication (IEMCON), pp 1–7
33. Esther Rani P, Shanmugalakshmi R (2014) Multimodal biometric system using score level fusion of palmprint and finger knuckle print. *Int J Adv Res Comput Sci* 5(6)
34. PolyU (2010) The Hong Kong polytechnic university (PolyU) Finger-Knuckle-Print Database, [Online]. Available: <http://www.comp.polyu.edu.hk/biometrics/FKP.html>
35. Usha K, Ezhilarasan M (2016) Personal recognition using finger knuckle shape oriented features and texture analysis. *J King Saud Univ Inf Sci* 28(4):416–431
36. Usha K, Ezhilarasan M (2016) Fusion of geometric and texture features for finger knuckle surface recognition. *Alex Eng J* 55(1):683–697
37. Vasan D, Alazab M, Wassan S, Naeem H, Safaei B, Zheng Q (2020) IMCFN: Image-based malware classification using fine-tuned convolutional neural network architecture. *Comput Netw* 171:107138
38. Veluchamy S, Karlmarx LR (2020) HE-Co-HOG and k-SVM classifier for finger knuckle and palm print-based multimodal biometric recognition. *Sens Rev*
39. Xinshao W, Cheng C (2015) Weed seeds classification based on PCANet deep learning baseline. In: 2015 Asia-Pacific Signal and Information Processing Association Annual Summit and Conference (APSIPA), pp 408–415
40. Zhang D, Kong W-K, You J, Wong M (2003) Online palmprint identification. *IEEE Trans Pattern Anal Mach Intell* 25(9):1041–1050
41. Zhang L, Zhang L, Zhang D, Zhu H (2010) Online finger-knuckle-print verification for personal authentication. *Pattern Recognit* 43(7):2560–2571
42. Zhu L, Zhang S (2010) Multimodal biometric identification system based on finger geometry, knuckle print and palm print. *Pattern Recognit Lett* 31(12):1641–1649

**Publisher's note** Springer Nature remains neutral with regard to jurisdictional claims in published maps and institutional affiliations.